

## BIOLOGICAL PROPERTIES OF Fe<sub>1.7</sub>Cr<sub>0.3</sub>O<sub>3</sub> NANOPARTICLES

Aele Manohar and K. Suresh Babu\*, Mohammad Gousuddin

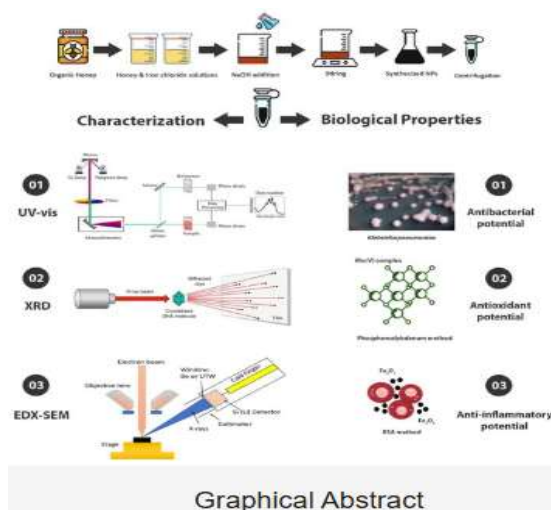
Lincoln university College, Malaysia

Corresponding author: K. Suresh Babu, Lincoln university College, Malaysia.

### ABSTRACT

Innovative methods for synthesizing nanoparticles have surfaced, offering eco-friendly, cost-effective, and biocompatible options to tackle the problem of drug resistance in microbes. The antibacterial efficacy against Fe<sub>1.7</sub>Cr<sub>0.3</sub>O<sub>3</sub> NPs, an opportunistic multidrug-resistant (MDR) pathogen, has not been investigated despite the recent introduction of using as a green source to manufacture Fe<sub>1.7</sub>Cr<sub>0.3</sub>O<sub>3</sub> NPs. Thus, in order to synthesize Fe<sub>1.7</sub>Cr<sub>0.3</sub>O<sub>3</sub> NPs, this work used a reducing and capping agent. The antibacterial, antioxidant, along with anti-inflammatory capabilities of the nanoparticles were evaluated after their characterisation. At 350 nm, the study using UV-Vis spectroscopy showed that there was an absorption band associated with the SPR peak. The crystalline structure of the Fe<sub>1.7</sub>Cr<sub>0.3</sub>O<sub>3</sub> NPs was verified by XRD analysis, this further established that 36.2 nm was the size of the crystal. The nanoparticles' iron and oxygen compositions were determined using electron dispersive X-ray spectroscopy. After additional trace elements (<1 ppm) and sodium (1.49 ppm) have been added, the ICP-MS results showed that iron had the greatest concentration at 87.15 ppm. The VSM study showed that the Fe<sub>1.7</sub>Cr<sub>0.3</sub>O<sub>3</sub> NPs have modest magnetic characteristics. Electron microscopy (SEM) indicated the non-uniform spherical shape and size range of 100-150 nm for the Fe<sub>1.7</sub>Cr<sub>0.3</sub>O<sub>3</sub> NPs. Thirty clinically isolated forms of Fe<sub>1.7</sub>Cr<sub>0.3</sub>O<sub>3</sub> NPs were tested for antibacterial activity of Fe<sub>1.7</sub>Cr<sub>0.3</sub>O<sub>3</sub> NPs, with a maximum inhibition zone of 10 mm. Thirty µg/mL was the MIC measurement for Fe<sub>1.7</sub>Cr<sub>0.3</sub>O<sub>3</sub> NPs. Nevertheless, no antibacterial effect was seen when Fe<sub>1.7</sub>Cr<sub>0.3</sub>O<sub>3</sub> NPs were mixed with three chosen antibiotics. Significant anti-inflammatory (IC<sub>50</sub> = 70 µg/mL) and antioxidant (IC<sub>50</sub> = 22 µg/mL) effects of Fe<sub>1.7</sub>Cr<sub>0.3</sub>O<sub>3</sub> NPs were seen at different doses when compared to the standard. Fe<sub>1.7</sub>Cr<sub>0.3</sub>O<sub>3</sub> NPs production might be investigated for potential biological uses and could replace conventional antibacterial medications.

**KEYWORDS:** Fe<sub>1.7</sub>Cr<sub>0.3</sub>O<sub>3</sub> NPs; Biological properties; Anti-inflammatory, Antioxidant, Anti-bacterial.



## INTRODUCTION

Because of its wide range of potential scientific uses, nanotechnology has garnered a great deal of interest during the last 20 years. Because of their little size often less than 100 nm the adaptability of nanoparticles stands out. Nanoparticles' reduced size influences a number of their characteristics, such as their surface area, magnetic and electrochemical capabilities, and more (Baimler et al., 2020). The use of nanotechnology in organic product synthesis is a rapidly developing field due to the many advantages that nanotechnology provides for the natural administration of medications, which may alleviate long-term health problems. The distinctive properties of metal oxide nanoparticles have recently attracted a great deal of research interest (Gopu et al., 2021). Applications such as medication administration, magnetic resonance imaging, as well as bioremediation are centered upon magnetic nanoparticles of metals, namely iron oxide nanoparticles ( $\text{Fe}_{1.7}\text{Cr}_{0.3}\text{O}_3$  NPs), which have been shown to be both biologically strong and biocompatible. Limonite ( $\text{Fe}_2\text{O}_3 \cdot \text{H}_2\text{O}$ ), hematite ( $\text{Fe}_2\text{O}_3$ ), and magnetite ( $\text{Fe}_3\text{O}_4$ ) are iron oxides that are most often seen. Emulsion processes, microemulsions, pyrolysis, non-aqueous methods, colloidal procedures, sol-gel methods, sonochemistry, co-precipitation of  $\text{Fe}^{2+}$  ions, and other chemical methods may be used to produce  $\text{Fe}_{1.7}\text{Cr}_{0.3}\text{O}_3$  NPs. Dangerous substances are a byproduct of these processes. Therefore, the employment of microorganisms and environmentally friendly methods in the production of  $\text{Fe}_{1.7}\text{Cr}_{0.3}\text{O}_3$  NPs has become more attractive (Shah et al., 2020).

Synthesis of  $\text{Fe}_{1.7}\text{Cr}_{0.3}\text{O}_3$  NPs was reported to be successful in a recent work. There have been further reports of the synthesis of  $\text{Fe}_{1.7}\text{Cr}_{0.3}\text{O}_3$  NPs in recent research as well. A combination of sugars, terpenoids and polyphenols, all alkaloid compounds, phenolic acids, and proteins gives natural extracts their reducing and capping abilities

and guarantees the structure of the nanoparticles is maintained steadily. Nanoparticle production may be greatly aided by functional groups such as “C-O-C, C-O, C=C, and C=O” which are included in these substances, according to the research. There has been medicinal usage of Fe<sub>1.7</sub>Cr<sub>0.3</sub>O<sub>3</sub> NPs since ancient times (Neupane et al., 2019). Nanoparticles may be synthesized with the help of Fe<sub>1.7</sub>Cr<sub>0.3</sub>O<sub>3</sub> NPs, an organic, naturally occurring nutrient source that includes substances that stabilize and reduce the synthesis process. Synthesis of Fe<sub>1.7</sub>Cr<sub>0.3</sub>O<sub>3</sub> NPs does not result in the release of any toxic by-products that might endanger human health when used to medical fields. Green synthesis using Fe<sub>1.7</sub>Cr<sub>0.3</sub>O<sub>3</sub> NPs is also a simple, fast, and biocompatible way to make several useful chemicals for many different uses. The effective production of biogenic Fe<sub>1.7</sub>Cr<sub>0.3</sub>O<sub>3</sub> NPs has been the subject of many recent publications (Rostamizadeh et al., 2020).

Not long ago, scientists found that Fe<sub>1.7</sub>Cr<sub>0.3</sub>O<sub>3</sub> NPs have potent antibacterial characteristics against a range of microorganisms, including “*P. aeruginosa*, *B. subtilis*, *S. aureus*, *E. coli*, *Penicillium* spp., as well as *Aspergillus* spp”. Different research found that *Oscillatoria limnetica* may be used to successfully synthesize Fe<sub>1.7</sub>Cr<sub>0.3</sub>O<sub>3</sub> NPs. While testing Fe<sub>1.7</sub>Cr<sub>0.3</sub>O<sub>3</sub> NPs against multidrug-resistant *Escherichia coli*, *Staphylococcus aureus*, and *Bacillus subtilis*, researchers found that they were very effective. Similarly, gum extract from *Bombax malabaricum* was an excellent means of producing Fe<sub>1.7</sub>Cr<sub>0.3</sub>O<sub>3</sub> NPs. It was shown that the production of Fe<sub>1.7</sub>Cr<sub>0.3</sub>O<sub>3</sub> NPs was caused by the bioactive compounds as well as phytochemicals found in the gum extract of Fe<sub>1.7</sub>Cr<sub>0.3</sub>O<sub>3</sub> NPs (Ali et al., 2023). When put to the test against “*S. aureus*, *B. halodurans*, and *M. luteus*”, the created NPs showed impressive antibacterial activity, according to the study. Since the emergence of bacteria and other organisms resistant to antibiotics has emerged as a major threat to human health throughout the world, the antimicrobial properties of Fe<sub>1.7</sub>Cr<sub>0.3</sub>O<sub>3</sub> NPs are more important than ever. The capacity of Fe<sub>1.7</sub>Cr<sub>0.3</sub>O<sub>3</sub> NPs to produce extremely reactive oxygen compounds has led to their effectiveness against several pathogenic bacteria. The morphological and physiological properties of Fe<sub>1.7</sub>Cr<sub>0.3</sub>O<sub>3</sub> NPs are thought to be the primary factors relating to their antibacterial action (Tufani et al., 2021).

In immunocompromised people, including those with diabetes, premature babies, or cancer, the opportunistic bacterium *Klebsiella pneumoniae* may cause a wide range of illnesses. The emergence of very dangerous Fe<sub>1.7</sub>Cr<sub>0.3</sub>O<sub>3</sub> NPs strains and the subsequent rise in medication resistance have resulted in a 42% mortality rate among both patients as well as healthy individuals (Lozhkomoev et al., 2021). Researchers are unaware of any previous evaluation of the in vitro antibacterial activity of Fe<sub>1.7</sub>Cr<sub>0.3</sub>O<sub>3</sub> NPs, particularly against the clinical isolates of Fe<sub>1.7</sub>Cr<sub>0.3</sub>O<sub>3</sub> NPs. Therefore, this study used sodium hydroxide and iron chloride hexahydrate (FeCl<sub>3</sub>•6H<sub>2</sub>O) to create Fe<sub>1.7</sub>Cr<sub>0.3</sub>O<sub>3</sub> NPs, using for its stabilizing and lowering properties. In addition, biogenic nanoparticles were characterized using a variety of methods, and their antioxidant, anti-inflammatory, and antibacterial properties were assessed (Gudkov et al., 2021).

## EXPERIMENTAL DETAILS

**Figure 1: Visual observation of color change from yellow to intense black during synthesis of Fe<sub>1.7</sub>Cr<sub>0.3</sub>O<sub>3</sub> NPs**

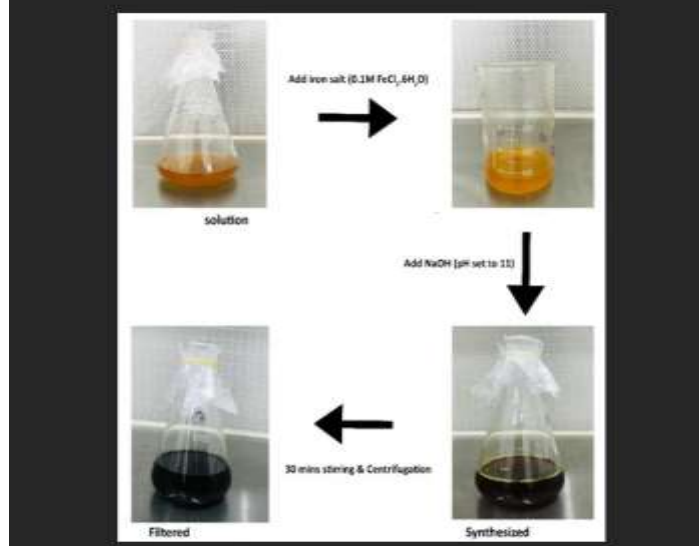
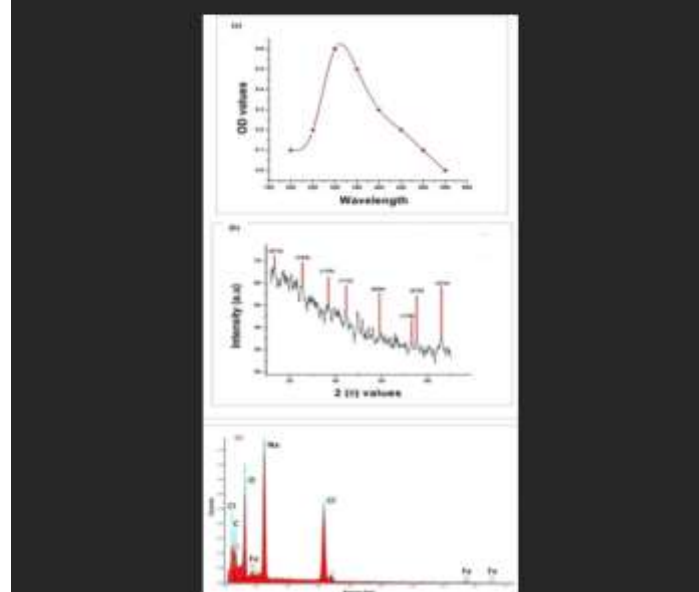


**Figure 2: Results representing the characterization of biogenic Fe<sub>1.7</sub>Cr<sub>0.3</sub>O<sub>3</sub> NPs. (a) UV-visible graph (a sharp peak at 350 nm is attributed to Fe<sub>1.7</sub>Cr<sub>0.3</sub>O<sub>3</sub> NPs); (b) XRD graph (highlighted peaks are attributed to crystalline nature of Fe<sub>1.7</sub>Cr<sub>0.3</sub>O<sub>3</sub> NPs); (c) EDX graph (clear Fe and O peaks)**



In this investigation, the first step in making Fe<sub>1.7</sub>Cr<sub>0.3</sub>O<sub>3</sub> NPs was to add NaOH to a solution of iron both sodium and salt hydroxide, stirring constantly. One way to visually identify nanoparticles in a solution is by looking for their development of a strong black hue (Figure 1). As a first step, researchers used UV-Vi's spectroscopy to validate that the produced Fe<sub>1.7</sub>Cr<sub>0.3</sub>O<sub>3</sub> NPs had surface plasmon resonance; the results indicated a strong peak at 350 nm (Figure 2a).

#### CHARACTERIZATION by XRD, SEM, EDX, ICP-MS AND VSM

Researchers used XRD analysis to find out whether the nanoparticles were crystalline and if they were single phase. For Fe<sub>1.7</sub>Cr<sub>0.3</sub>O<sub>3</sub> NPs, identified as  $2\theta$  values of  $24.68^\circ$ ,  $33.88^\circ$ ,  $38.44^\circ$ ,  $41.36^\circ$ ,  $49.8^\circ$ ,  $56.64^\circ$ ,  $57.48^\circ$ , or  $62.88^\circ$ , respectively, the figures reveal prominent peaks that correlate to index values of "(012), (104), (110), (113), (024), (116), (018), along with (214)", respectively. When these results were contrasted with the Fe<sub>1.7</sub>Cr<sub>0.3</sub>O<sub>3</sub> NPs value given by "the Joint Committee on Experts of Powder Diffraction Standard (JCPDS No. 24-0072)", many interesting patterns were apparent. The crystal planes demonstrated the crystalline structure of the Fe<sub>1.7</sub>Cr<sub>0.3</sub>O<sub>3</sub> NPs in the sample, with a mean lattice stress of 0.00285 and the Debye-Scherrer equation integrated ( $D = K \lambda / B1/2 \cos b$ ) led to the determination of an average crystal size of 36.2 nm. Crystal planes with a lattice constant of  $a = b = 5.0346 \text{ \AA}$  or  $c = 13.7473 \text{ \AA}$  indicate that the Fe<sub>1.7</sub>Cr<sub>0.3</sub>O<sub>3</sub> NPs that were generated could be found in a rhombohedral crystalline phase. Coordinates for these lattice constants were found in the "Crystallography Open Database (COD No. 9015964)". The EDX analysis findings are shown in Figure 2c, which revealed the chemical structure of the solution containing the Fe<sub>1.7</sub>Cr<sub>0.3</sub>O<sub>3</sub> NPs. With the use of K- $\alpha$  peaks observed between 0.0 as well as 0.83 keV, researchers were able to confirm that the generated nanoparticles included Fe and O. The nanoparticles are iron oxide, as shown by the presence of oxygen. The presence of the nanoparticle production was validated by the peaks of carbon and oxygen atoms. Additionally, ions of sodium and chloride were found to be present in the solution. According to Table 1, the primary component in this investigation was Fe<sub>1.7</sub>Cr<sub>0.3</sub>O<sub>3</sub> NPs, as the EDX spectra showed the largest amount of Fe elements.

**Table 1: The elemental composition of synthesized Fe<sub>1.7</sub>Cr<sub>0.3</sub>O<sub>3</sub> NPs as per the EDX analysis**

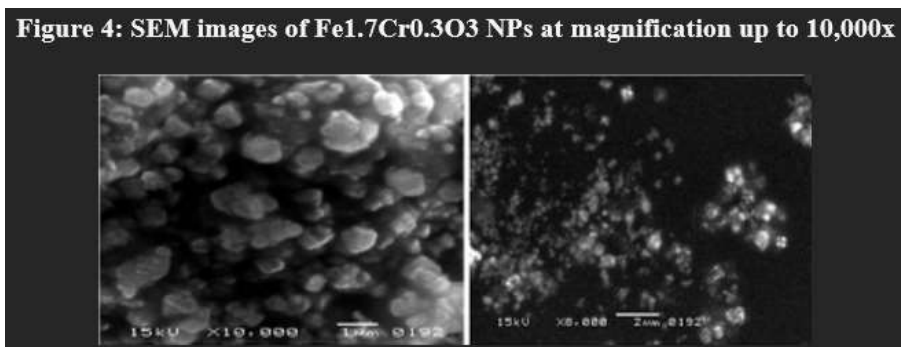
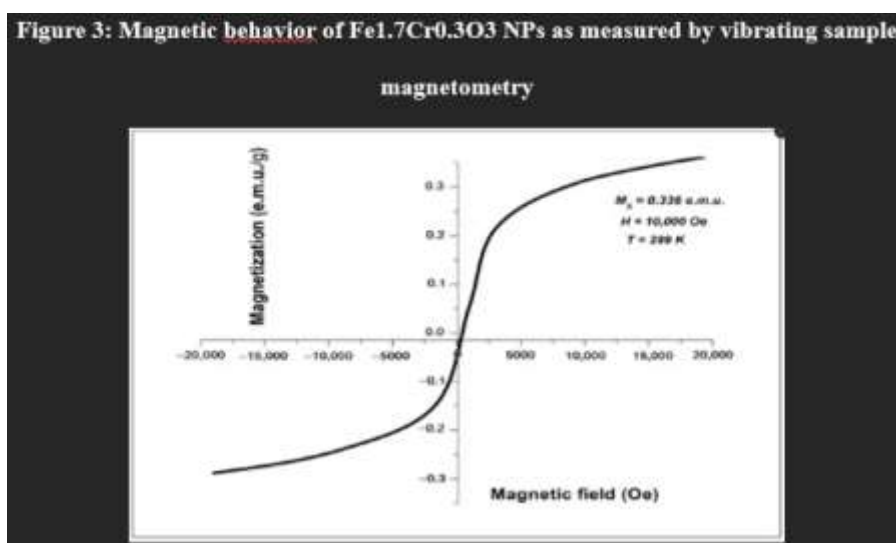
Element	Weight %	Atomic %	Net Int.
Fe O	40.73	50.48	363.77
Na Cl	7.58	4.87	40.73

To find out how much of each trace element existed in the produced Fe<sub>1.7</sub>Cr<sub>0.3</sub>O<sub>3</sub> NPs, researchers ran an ICP-MS study. Using a spectrum of wavelengths, the concentration of every detectable element was measured in parts per million. Various wavelengths and intensities were found to detect the maximum amounts of Fe and Na, as shown in Table 2. The concentration of sodium was 1.49 ppm, and its wavelength was 589.590 nm, with a wavelength of 762,552.31 c/s. The wavelength of iron was 238.204 nm, and its brightness was 508.64 c/s.

**Table 2: The trace element composition of synthesized Fe<sub>1.7</sub>Cr<sub>0.3</sub>O<sub>3</sub> NPs as per the ICP-MS analysis**

Trace Elements	Wavelength (nm)	Concentration (ppm)
Fe	238.204	87.15
Na	589.590	1.49
As	188.980	0.02
Cd	214.439	0.09
Co	238.892	0.03
Cr	267.716	0.02
Cu	327.395	-0.03
Mg	279.553	0.02
Mn	257.610	0.02
Ni	231.604	0.07
Pb	220.353	0.06
Zn	213.857	0.02
Se	196.026	0.02

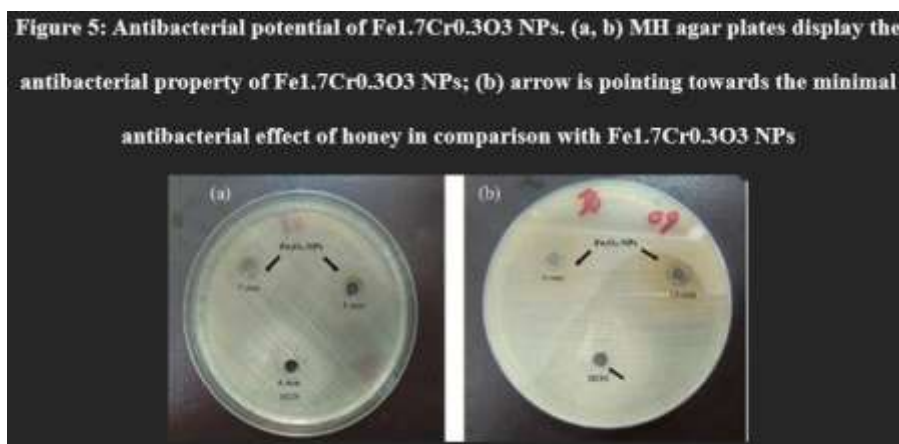
The synthesised hematite Fe<sub>1.7</sub>Cr<sub>0.3</sub>O<sub>3</sub> NPs magnetic resonance loop (MH-loop) at 299 K is shown in Figure 3. A saturated magnetization ( $M_s$ ) value of “0.336 e.m.u./g at 1 Tesla (10,000 Oe)” demonstrated the weak ferromagnetic property of the produced Fe<sub>1.7</sub>Cr<sub>0.3</sub>O<sub>3</sub> NPs, as shown by the function. Using scanning electron microscopy (SEM), Figure 4 shows the microscopic (size and form) characteristics of the Fe<sub>1.7</sub>Cr<sub>0.3</sub>O<sub>3</sub> NPs that were created. The formation of evenly dispersed nanostructures in the solution was verified by these pictures. The manufactured Fe<sub>1.7</sub>Cr<sub>0.3</sub>O<sub>3</sub> NPs showed a constant fluctuation in size and form. The non-uniform spherical shape of the Fe<sub>1.7</sub>Cr<sub>0.3</sub>O<sub>3</sub> NPs size distribution was calculated to be in the frequency range of 100-200 nm at 19,000x magnification.



## ANTI-BACTERIAL ACTIVITY



Here, researchers examine in depth how freshly produced Fe<sub>1.7</sub>Cr<sub>0.3</sub>O<sub>3</sub> NPs inhibit the growth of the infamous opportunist Gram-negative bacteria, Fe<sub>1.7</sub>Cr<sub>0.3</sub>O<sub>3</sub> NPs. Figure 5a displays the measured zone widths, which indicate that a 30 µg/mL dosage of Fe<sub>1.7</sub>Cr<sub>0.3</sub>O<sub>3</sub> NPs had the strongest shown antimicrobial efficacy against every single strain in vitro. When applied alone, the solution failed to kill bacteria (Figure 5b) since no inhibition zones were visible. A 10 mm inhibition zone was seen against “HS-K4, HS-K-5, HS-K9, and HS-K-15, the greatest of all the isolates. However, HS-K-17 and HS-K-19” showed the smallest inhibitory zone, measuring just 5 mm. The remaining twenty-four Fe<sub>1.7</sub>Cr<sub>0.3</sub>O<sub>3</sub> NPs isolates showed intermediate values, ranging from 6 mm to 9 mm.



The ELISA reader absorbance data were used to determine that the produced Fe<sub>1.7</sub>Cr<sub>0.3</sub>O<sub>3</sub> NPs had a MIC value of 30 µg/mL. Following incubation, antibiotics were tested in vitro against clinical forms of Fe<sub>1.7</sub>Cr<sub>0.3</sub>O<sub>3</sub> NPs to determine their effectiveness. Researchers also compared the combined antibacterial properties of nanoparticles and three medications to their separate antibacterial potential and evaluated the results. All strains of Fe<sub>1.7</sub>Cr<sub>0.3</sub>O<sub>3</sub> NPs exhibited sensitivity (S) to CIP-5, whereas all of the strains showed some level of resistance (I) to CN-10 and FEP-30, according to the findings that were interpreted in accordance with CLSI recommendations. It is somewhat surprising that the combination of antibiotics and nanoparticles did not result in the appearance of any zones of inhibition.

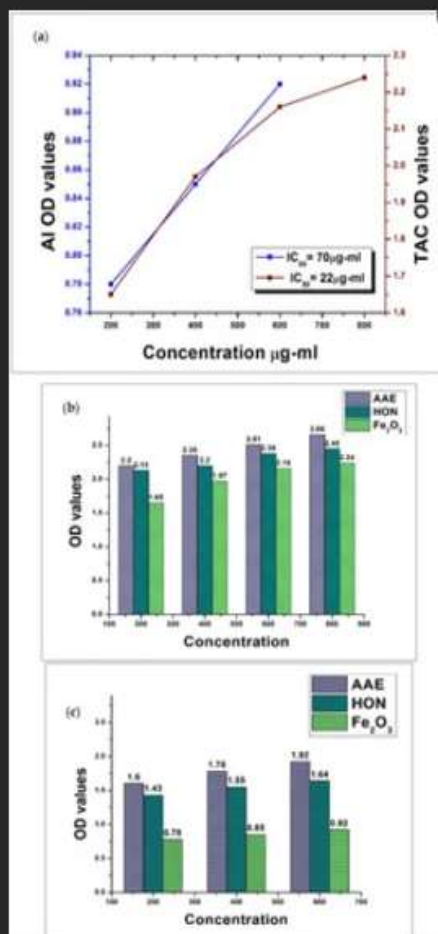
## ANTI-OXIDANT ACTIVITY

Compared to the gold standard, Fe<sub>1.7</sub>Cr<sub>0.3</sub>O<sub>3</sub> NPs had a far higher antioxidant capacity. The reflectance readings were taken at 200, 400, 600, and 800 µg/mL concentrations,



for Fe1.7Cr0.3O3 NPs were 1.65, 1.97, 2.16, and 2.24, correspondingly. Readouts of 2.2, 2.35, 2.51, along with 2.66 were obtained at the same concentrations of AAE that served as a reference. With doses of “200 µg/mL, 400 µg/mL, 600 µg/mL, and 800 µg/mL”, HON exhibited absorption values of 2.13, 2.2, 2.38, and 2.45, correspondingly. As shown in Figure 6a, the IC50 value for Fe1.7Cr0.3O3 NPs was found in the range of 22 µg/mL when produced as a result of how “total antioxidant capacity (TAC)”. Figure 6b also showed that the antioxidant capability of the sample increased with the concentration of nanoparticles.

**Figure 6: Antioxidant and anti-inflammatory potential of Fe1.7Cr0.3O3 NPs. (a) IC50 values for total antioxidant capacity (TAC) and anti-inflammatory (AI) activity of Fe1.7Cr0.3O3 NPs in terms of ascorbic acid (AAE) and honey (HON); (b) TAC values for different concentrations of Fe1.7Cr0.3O3 NPs in terms of AAE and HON; (c) AI values for different concentrations of Fe1.7Cr0.3O3 NPs in terms of AAE and HON**



## ANTI-INFLAMMATORY ACTIVITY

When compared to the gold standard, Fe<sub>1.7</sub>Cr<sub>0.3</sub>O<sub>3</sub> NPs showed far stronger anti-inflammatory potential. At doses of 200, 400, along with 600 µg/mL, the produced nanoparticles showed absorbance coefficients of 0.78, 0.85, and 0.92, respectively. Contrarily, it was shown that AAE had absorption values of 1.6, 1.78, then 1.92 at the same quantities, whereas HON had spectrophotometer readings of 1.43, 1.55, and 1.64 at “200 µg/mL, 400 µg/mL, or 600 µg/mL”, respectively. Its anti-inflammatory (AI) potential, Figure 6a shows that the IC<sub>50</sub> value for Fe<sub>2</sub>O<sub>3</sub>-NPs was determined to be 70 µg/mL. As the concentration of Fe<sub>1.7</sub>Cr<sub>0.3</sub>O<sub>3</sub> NPs in the solution rose, the anti-inflammatory ability also increased, as shown in Figure 6c, the graph.

## CONCLUSION

Because of its many uses in fields as diverse as health, electronics, the environment, and industry, nanotechnology has recently grown into a fast-developing scientific discipline. The current study used organic solution as a green manufacturing method for iron oxide nanoparticles; this strategy is safe, sustainable, nontoxic, conveniently available, and cost-effective. This study's manufactured Fe<sub>1.7</sub>Cr<sub>0.3</sub>O<sub>3</sub> NPs are more stable as chemically generated nanoparticles because the phytochemical components on the particles surface reduce the likelihood of clumping. They also have the added benefit of not requiring as much time-consuming and labour-intensive centrifugation as other metal nanoparticles made of oxide when it comes to separation. Moreover, when tested against Fe<sub>1.7</sub>Cr<sub>0.3</sub>O<sub>3</sub> NPs that had been obtained from clinical settings, these nanoparticles demonstrated strong antibacterial, antioxidant, along with anti-inflammatory properties. Put together, these characteristics render them strong contenders for antibacterial drugs that might have great potential in the biomedical field.

## REFERENCES

1. Ali, I.; Pan, Y.; Jamil, Y.; Chen, J.; Shah, A.A.; Imran, M.; Alvi, U.; Nasir, N.; Shen, Z. Hybrid Au/Co nanoparticles: Laser-assisted synthesis and applications in magnetic hyperthermia. *Phys. B: Condens. Matter* 2023, 657, 414773.
2. Baimler, I.V.; Lisitsyn, A.B.; Gudkov, S.V. Water decomposition occurring during laser breakdown of aqueous solutions containing individual gold, zirconium, molybdenum, iron, or nickel nanoparticles. *Front. Phys.* 2020, 8, 620938.

3. Gopu, M.; Kumar, P.; Selvankumar, T.; Senthilkumar, B.; Sudhakar, C.; Govarthanan, M.; Selvam, K. Green biomimetic silver nanoparticles utilizing the red algae *Amphiroa rigida* and its potent antibacterial, cytotoxicity, and larvicidal efficiency. *Bioprocess Biosyst. Eng.* 2021, 44, 217-223.
4. Gudkov, S.V.; Burmistrov, D.E.; Serov, D.A.; Rebezov, M.B.; Semenova, A.A.; Lisitsyn, A.B. Do iron oxide nanoparticles have significant antibacterial properties? *Antibiotics* 2021, 10, 884.
5. Lozhkomoev, A.; Pervikov, A.; Kazantsev, S.; Sharipova, A.; Rodkevich, N.; Toropkov, N.; Lerner, M. Synthesis of Fe/Fe<sub>3</sub>O<sub>4</sub> core-shell nanoparticles by electrical explosion of the iron wire in an oxygen-containing atmosphere. *J. Nanoparticle Res.* 2021, 23, 73.
6. Neupane, B.P.; Chaudhary, D.; Paudel, S.; Timsina, S.; Chapagain, B.; Jamarkattel, N.; Tiwari, B.R. Himalayan honey-loaded iron oxide nanoparticles: Synthesis, characterization, and study of antioxidant and antimicrobial activities. *Int. J. Nanomed.* 2019, 14, 3533.
7. Rostamizadeh, E.; Iranbakhsh, A.; Majd, A.; Arbabian, S.; Mehregan, I. Green synthesis of Fe<sub>2</sub>O<sub>3</sub> nanoparticles using fruit extract of *Cornus mas* L. and its growth-promoting roles in barley. *J. Nanostructure Chem.* 2020, 10, 125-130.
8. Shah, A.A.; Bhatti, M.A.; Tahira, A.; Chandio, A.D.; Channa, I.A.; Sahito, A.G.; Chalangar, E.; Willander, M.; Nur, O.; Ibupoto, Z.H. Facile synthesis of copper-doped ZnO nanorods for the efficient photodegradation of methylene blue and methyl orange. *Ceram. Int.* 2020, 46, 9997-10005.
9. Tufani, A.; Qureshi, A.; Niazi, J.H. Iron oxide nanoparticles-based magnetic luminescent quantum dots (MQDs) synthesis and biomedical/biological applications: A review. *Mater. Sci. Eng. C* 2021, 118, 111545.